Journal of Materials Chemistry B

In situ crosslinking of electrospun gelatin for improved fiber morphology retention and tunable degradation

Journal:	*Journal of Materials Chemistry B*
Manuscript ID:	TB-ART-05-2015-000937.R1
Article Type:	Paper
Date Submitted by the Author:	24-Jul-2015

Complete List of Authors:	Kishan, Alysha; Texas A&M University, Biomedical Engineering Nezarati, Roya; Texas A&M University, Biomedical Engineering Radzicki, Christopher; Texas A&M University, Biomedical Engineering Renfro, Audrey; Texas A&M University, Biomedical Engineering Robinson, Jennifer; Texas A&M University, Biomedical Engineering Whitely, Michael; Texas A&M University, Biomedical Engineering Cosgriff-Hernandez, Elizabeth; Texas A&M University, Biomedical Engineering

Journal of Materials Chemistry B

ARTICLE

In situ crosslinking of electrospun gelatin for improved fiber morphology retention and tunable degradation

Received 00th January 20xx,
Accepted 00th January 20xx

DOI: 10.1039/x0xx00000x

www.rsc.org/

A. P. Kishan,*[a] R. M. Nezarati,*[a] C. M. Radzicki,[a] A. L. Renfro,[a] J. L. Robinson,[a] M. Whitely[a] and E. Cosgriff-Hernandez[a+]

Electrospinning is a popular technique to fabricate tissue engineering scaffolds due to the exceptional tunability of the fiber morphology, which can be used to control the scaffold mechanical properties, degradation rate, and cell behavior. Recent work has focused on electrospinning natural polymers such as gelatin to improve the regeneration potential of these grafts. Gelatin scaffolds must be crosslinked to avoid rapid dissolution upon implantation with current crosslinking strategies requiring additional post-processing steps. Despite the strong dependence of scaffold properties on fiber morphology, there has been minimal emphasis on retaining the original fiber morphology of electrospun gelatin scaffolds after implantation. This work describes a method for *in situ* crosslinking of gelatin to produce electrospun fibers with improved fiber morphology retention after implantation. A double barrel syringe with an attached mixing head and a diisocyanate crosslinker were utilized to generate electrospun scaffolds that crosslink during the electrospinning process. These *in situ* crosslinked fiber meshes retained morphology after 1 week incubation in water at 37°C; whereas, uncrosslinked meshes lost the fibrous morphology within 24 hours. Degree of crosslinking was quantified and relationships between the crosslinker ratio and enzymatic degradation rate were evaluated. The degradation rate decreased with increased crosslinker ratio, resulting in a highly tunable system. Additionally, tensile testing under simulated physiological conditions indicated that increased crosslinker ratios resulted in increases in initial modulus and tensile strength. Overall, this *in situ* crosslinking technique provides a method to crosslink gelatin during electrospinning and can be used to tune the degradation rate of resulting scaffolds while enabling improved fiber morphology retention after implantation.

Introduction

Electrospinning has gained popularity in recent years as a technique to fabricate nonwoven, fibrous scaffolds with high porosities, large surface area-to-volume ratios, and nano- to micron-sized fiber diameters.[1-3] To generate these scaffolds, a polymer solution is pumped at a constant rate through a needle tip that is placed a set distance away from a grounded or oppositely charged collector. When a voltage is applied at the needle tip, the droplet erupts into a liquid jet that narrows and solidifies during flight to be collected as a fiber.[3] The relative ease of modulating the fiber architecture through variation of processing, solution, or environmental parameters provides a means to tune cell behavior, degradation rate, and mechanical properties. For example, fiber alignment and fiber diameter have been shown to strongly influence mechanical properties.[4-7] As a result, control over electrospun fiber morphology is an important factor in scaffold design. By utilizing the high tunability of electrospun scaffolds, properties can be tailored to meet specific design criteria of a variety of clinical applications.

To improve the regeneration potential of electrospun grafts, research has focused on the development of methods to utilize bioactive materials that promote and guide cell growth and differentiation. Bioactive materials have a positive effect on living cells and include minerals, growth factors, and proteins/peptides. Gelatin, a natural polymer derived from collagen, has been widely utilized in tissue engineering due its demonstrated ability to enhance cell adhesion and proliferation.[8, 9] Crosslinking of gelatin is necessary for implementation as a tissue engineering scaffold to prevent rapid dissolution and retain the three dimensional structure. The most commonly implemented technique for crosslinking gelatin is via exposure to glutaraldehyde vapor. Although widely used, glutaraldehyde has associated risks of toxic residues[10-12] and calcification *in vivo*.[13-15] Glutaraldehyde crosslinking of gelatin fibers and subsequent immersion in water typically results in swelling and loss of fiber architecture unless high concentrations are used, which can contribute to an increased risk of toxicity.[10, 16] To overcome these limitations, 1-ethyl-3-(3-dimethylaminopropyl)carbodiimide hydrochloride (EDC) has

* *Co-first authors*

[a] *Department of Biomedical Engineering, Texas A&M University, College Station, Texas 77843-3120, USA*

+ *Corresponding Author*

been investigated and is advantageous as a zero-length crosslinking agent.[17, 18] Genipen, a molecule isolated from gardenia fruits, has also been utilized for crosslinking of natural polymers and has displayed a greater biocompatibility than glutaraldehyde.[19, 20] Significant work has been devoted to improving the biocompatibility of crosslinked gelatin; however, there has been minimal emphasis on retaining the original fiber morphology of electrospun gelatin scaffolds post-crosslinking. Numerous researchers report enlarged, swollen, and/or fused fibers after the chosen crosslinking procedure.[21-23]

In addition to maintaining fiber morphology after the crosslinking process, maintaining the morphology of electrospun fibers upon immersion in aqueous environments is of great importance. Fiber morphology has been shown to have a direct impact upon cell culture, ranging from impacting the orientation of cells to regulating differentiation. Cell behavior can be controlled via contact guidance of electropun fibers, which can play a key role in mimicking the complex and hierarchical structure of many tissues. The ability to control the structure of the cells via topography can aid in the regeneration of functional tissues. For example, aligned cells are a key requirement in neural tissue engineering.[24] Schwann cells cultured on aligned fiber scaffolds have been shown to orient in the direction of the fibers due to contact guidance. The nucleus and focal adhesion molecule vinculin also aligned along the fiber direction and increased proliferation was observed as compared to random meshes. Additionally, these topographic cues were shown to direct Schwann cells towards the pro-myelinating state, as indicated by the markers for myelin-specific genes MAG, P0, MBP, and PMP22.[24] Fiber alignment has also been investigated for the regeneration of the anterior cruciate ligament. Significantly more collagen was synthesized on aligned nanofiber sheets resulting in spindle-shaped, oriented cells with morphology similar to ligament fibroblasts *in vivo*.[25] In addition to alignment, the effect of fiber diameter on spreading, proliferation, and differentiation of osteoblastic cells, fibroblasts and neural stem cells has been investigated by Badami et al, Bashur et al, and Christopherson et al, respectively.[26-28] Given the well established impact of fiber morphology on scaffold mechanical properties, degradation rate, and cell behavior, the retention of fiber morphology post-implantation is necessary for the design of scaffolds with predictable properties and cellular response.

This work describes a method for *in situ* crosslinking of gelatin to fabricate electrospun meshes with controlled degradation to direct tissue regeneration and improve fiber morphology retention upon implantation. A double barrel syringe with an attached mixing head and a diisocyanate crosslinker were utilized to generate these scaffolds, as depicted in Figure 1. The degree of crosslinking was assessed to confirm and quantify successful crosslinking, and scanning electron microscopy was used to characterize the overall fiber morphology. The effects of increasing the crosslinker ratio on tensile properties and fiber morphology after immersion in water, in comparison to traditional glutaraldehyde vapor crosslinked meshes, were investigated. An *in vitro* degradation model utilizing collagenase solution was employed to characterize the effect of crosslinker ratio on degradation rate. Finally, human mesenchymal stem cell adhesion on meshes was quantified to evaluate potential of the meshes as tissue engineering scaffolds.

Experimental

Materials

All chemicals were purchased from Sigma-Aldrich and used as received unless otherwise stated.

Electrospinning

In situ crosslinking of electrospun gelatin was performed using double barrel syringes (1:1 barrel ratio) (Nordson EFD) with attachable mixing heads (3.1 mm ID x 53.5 mm length). One barrel was loaded with a 10 wt% solution of bovine-derived gelatin in 2,2,2-trifluoroethanol (TFE). A catalyst, 1,4-diazabicyclo[2,2,2]octane (DABCO), was added at 5 wt% of solids to the gelatin solution prior to loading the syringe. The second barrel was loaded with a solution of hexamethylene diisocyanate (HDI) in TFE. The concentration of HDI was varied such that the crosslinker density would equal a 1X, 5X, or 10X ratio of isocyanate/amine. For the crosslinker ratio calculations, 11 lysines per gelatin molecule were assumed. A blunted 18 gauge needle was attached via a Luer-Slip fitting onto the mixing head, and the syringe was placed in a syringe pump (KDS100, KDScientific) set to a constant flow rate of 1.0 mL/hr. A high voltage of 10 kV (ES30P-5W/DDPM, Gamma Scientific) was applied at the needle tip, and fibers were collected on a 6 cm square copper plate set 12 cm away from the needle tip. The front of the flat plate collector was covered with a thin latex film that facilitated removal of the mesh after deposition. Each mesh had a total collection time of 3 hours. Halfway through each run, the mixing head was replaced to avoid clogging due to crosslinking within the mixing head. Meshes were then placed under vacuum for 24 hours to remove any residual solvent.

Traditional glutaraldehyde crosslinked controls were fabricated by electrospinning uncrosslinked gelatin followed by vapor crosslinking. Briefly, 10 wt% solution of bovine-derived gelatin in TFE was loaded into a syringe and dispensed at 1.0 mL/hr. 10 kV was applied at the needle tip and a grounded copper plate collector was set 12 cm away from the needle tip. Each mesh had a total collection time of 3 hours. Crosslinking was then performed by incubating the meshes in vapor of glutaraldehyde for 24 hours.[25] The crosslinked meshes were then vacuumed overnight to remove any residual glutaraldehyde.

Degree of Crosslinking

Degree of crosslinking was determined for the electrospun gelatin meshes using a ninhydrin assay. The percentage of free amine groups in the gelatin mesh was quantified by their reaction with ninhydrin (2, 2-dihydroxy-, 3-indiandione).[29-31] Meshes of 5 mg were soaked in water for one hour. Specimens (n=3) were then heated with the ninhydrin reagent, phenol solution and potassium cyanide solution at 120°C for 5 minutes. The solution was then cooled to room temperature and diluted

with isopropyl alcohol. The optical absorbance of the solution was recorded using a plate reader (Spectramax M5, Molecular Devices) at 570 nm.[29] The absorbance of the solution is directly related to the amount of free amino groups in the sample after heating with ninhydrin. The degree of crosslinking was then calculated as the percent of bound amine groups using the equation below:

$$\textbf{\textit{Degree of Crosslinking}}\ (\%) = \left(1 - \frac{A_C}{A_U}\right) \times 100$$

A_C and A_U represent the absorbance of crosslinked and uncrosslinked gelatin meshes, respectively.[30]

Electrospinning Fiber Characterization

Specimens (n=4) approximately 7 mm square were cut from the center of each fiber mesh to avoid edge effects. The fiber morphology was observed using scanning electron microscopy (SEM, Phenom Pro, NanoScience Instruments) at 10 kV accelerating voltage. Prior to imaging, the specimens were coated with 4 nm of gold using a sputter coater (Sputter Coater 108, Cressingtion Scientific Instruments). Fiber characterization after immersion in water was performed by first cutting circular punches (10 mm diameter) and placing each on a glass coverslip in a well plate. The punches were then weighted to ensure immersion, and the wells were filled with reverse osmosis water. Specimens were stored at 37 °C and were removed at 24 h, 48 h, 72 h, and 1 week timepoints, frozen at -80 °C overnight, and lyophilized prior to imaging with SEM, as described above.

Tensile Testing

Dogbone specimens (n=4) were cut in accordance with ASTM D1708 and strained to failure at a rate of 100% per min based on the initial gauge length using an Instron 3345 uniaxial tensile tester equipped with a 100 N load cell and pneumatic side action grips (Instron 2712-019). Specimens were equilibrated in water at 37°C for 24 hours prior to testing. An environmental control chamber was attached such that simulated physiological conditions (37°C, 100% humidity to limit specimen drying) were maintained throughout testing. The elastic modulus, tensile strength, and ultimate elongation were calculated from the resultant engineering stress/strain curves. A secant modulus at 2% strain was calculated for the elastic modulus and subsequently referred to as "modulus."

Enzymatic *in vitro* Degradation

Enzymatic degradation of the *in situ* crosslinked gelatin meshes was performed using type 1 collagenase (349 U/mg). Electrospun specimens (40 x 10 x 0.2 mm^3) were placed into capped tubes containing 2 mL of 0.02 units collagenase/mL of PBS and incubated at 37 °C with shaking.[30, 32] Solutions were changed every 3 days. At each time point, specimens (n=3) were collected using centrifugation and carefully rinsed 3 times with distilled water. Samples were subsequently frozen overnight and then lyophilized. The mass loss of the degraded sample was determined after lyophilization by dividing the mass loss by the initial dry mass. Specimens removed at 1 week, 2 weeks, and 4 weeks were imaged with SEM after lyophlization.

Cell Viability and Adhesion

Bone marrow-derived human mesenchymal stem cells (hMSCs) were obtained as Passage 1 in a cryovial from the Center for the Preparation and Distribution of Adult Stem Cells. Cells were cultured in growth media containing 16.5% fetal bovine serum (FBS, Atlanta Biologicals), 1% L-glutamine (Life Technologies), and Minimum Essential Media α (MEM α, Life Technologies) to 80% confluency and utilized at Passage 6. Specimens were placed in a tissue cultured 48-well plate (Corning) and were UV sterilized for 2 hours. Cells were seeded at 10,000 cells/cm^2 in growth media supplemented with 1 vol% penicillin-streptomycin (Life Technologies) and cultured at 37°C and 5%CO_2 for 24 hours or 1 week. Viability of hMSCs on *in situ* crosslinked electrospun gelatin was conducted using the Live/Dead assay kit (Molecular Probes) to determine the material cytocompatibility in comparison to glutaraldhyde crosslinked fibers and tissue culture polystyrene (TCPS). Cells were washed with PBS, stained with calcein-AM and ethidium homodimer-1 for 30 minutes in 37 C, and replaced with PBS for imaging. Viability was then calculated from cell counts of images obtained through raster patterning (5 images per specimen) of 3 specimens (n = 15) using a confocal microscope (Nikon Eclipse TE2000-S). Cell adhesion at 24 hours and 1 week was assessed by fixing cells with 3.7% glutaraldehyde followed by staining with rhodamine phalloiding (F-actin/cytoplasm, Life Technologies) and SYBRGreen (DNA/nucleus, Life Technologies). Cell adhesion was calculated from cell counts of images obtained through raster patterning (5 images per specimen) of 3 specimens (n = 15) using a confocal microscope (Nikon Eclipse TE2000-S).

Statistical Analysis

The data are displayed as mean ± standard deviation for each composition. A Student's t-test was performed to determine any statistically significant differences between compositions. All tests were carried out at a 95% confidence interval ($p<0.05$).

Results and Discussion

Fiber Characterization

In situ crosslinking of electrospun gelatin was achieved using a double barrel syringe that enabled isolation of the individual gelatin and hexamethylene diisocyanate (HDI) crosslinker solutions until mixing through a mixing head, **Figure 1**. Tronci et al. utilized diisocyanate to crosslink gelatin foams and demonstrated that isocyanates react readily with the lysine residues of the gelatin, without heat, to form a disubstituted urea.[33] Several *in situ* crosslinking methods have been evaluated to provide a one-step crosslinking process for water-soluble polymers without post-processing. One *in situ* crosslinking approach involves the direct addition of crosslinkers such as glutaraldehyde and EDC-NHS to the electrospinning solution.[34, 35] However, as noted by Tang et al, these systems are limited by resulting time-dependent rheology and compatibility with

electrospinning. By directly mixing the polymer and crosslinking solutions, dynamic rheology analysis indicated that significant rheological changes (increase in viscosity) in the precursor solution occurred during the electrospinning process. As a result, this method of *in situ* crosslinking causes changes in fiber morphology in the resultant mesh, ranging from beaded fibers (low viscosity solutions) to large, flat fibers (very high viscosity solutions).[35] By utilizing a double barrel syringe to combine the crosslinker and polymer solution, the viscosity of the electrospinning solution is maintained as the two solutions only react upon exposure within the mixing head. The two solutions mix promptly before ejection through the needle tip, enabling this method to produce scaffolds with homogenous fiber morphology. Studies have also shown the efficacy of UV crosslinking during the electrospinning process.[36, 37] By exposing the fibers to UV light during the whipping process, this method provides the advantage of homogenous crosslinking, which is not seen with vapor-phase crosslinking (ex. Glutaraldehyde). However, the polymers must either contain specific functional groups for UV crosslinking (ex. acrylates, cinnamates) or the polymers must be mixed with crosslinkers containing UV activated structures such as phenyl azido groups.[36, 37] In addition to the extra cost of a UV set up, complicated chemistries are required to functionalize water-soluble polymers, as well as to synthesize UV activated structures. To the best of our knowledge, this is the first report of the use of a double barrel syringe to fabricate *in situ* crosslinked electrospun fibers.

Degree of crosslinking was determined by quantifying the amount of remaining free amines in the system through a ninhydrin assay. Ninhydrin readily reacts with free amines and produces a vivid purple hue upon reaction with free amine groups.[30] As depicted in **Table 1**, there was a direct increase in the degree of crosslinking with increased crosslinker ratio (isocyanate to amine). Additionally, glutaraldehyde vapor crosslinked meshes were calculated to have comparable degree of crosslinking to the 5X *in situ* crosslinked meshes. These results indicate that liquid phase crosslinking of electrospun gelatin imparts significant control over the crosslinking density, thus allowing for fabrication of meshes with specific crosslink densities.

The crosslinker ratio, and thus degree of crosslinking, was varied to evaluate the effect on fiber morphology retention, degradation rate, and mechanical properties. At each crosslinker ratio tested, smooth, uniform fibers with similar fiber diameters were electrospun. The average fiber diameter of the 1X mesh was 0.74 ± 0.32 μm, 5X was 0.77 ± 0.17 μm, and 10X was 0.72 ± 0.29 μm, **Table 1**. The fiber morphology after immersion in water for 1 week was characterized using SEM of lyophilized meshes, **Figure 2**. The uncrosslinked gelatin fibers immersed in water exhibited a morphology characteristic of freeze dried scaffolds, and the glutaraldehyde crosslinked fibers showed flattened and fused fibers indicative of partial dissolution. Large, flattened fibers, indicative of partial dissolution, were observed for the 1X gelatin fibers. The 5X and 10X meshes retained similar fiber diameters to their as-spun counterparts but with an increase in fiber fusion. The average fiber diameters after immersion for the 1X, 5X and 10X meshes were 2.42 ± 1.44 μm, 0.85 ± 0.25 μm, 0.89 ± 0.31 μm, respectively. The fiber diameter of the glutaraldehyde crosslinked fibers were calculated to be 1.15 ± 0.22 μm and 1.37 ± 0.41 μm before and after immersion, respectively. Compared with these controls, the 5X and 10X *in situ* crosslinked gelatin meshes demonstrated an improved retention of fiber morphology. Additionally, the similar degree of crosslinking of the 5X mesh and the glutaraldehyde crosslinked mesh (57% vs 61%) allowed for a comparison of the two crosslinking methods. There was an evident increase in fiber retention using the *in situ* crosslinking approach over vapor phase crosslinking. This was exhibited by an increase in fiber diameter of the glutaraldehyde crosslinked fibers after immersion (+19% vs +9%) and an increase in fiber fusion, as compared to the 5X meshes.

It is hypothesized that *in situ* crosslinking overcomes limitations of vapor crosslinking by initiating the crosslinking prior to the solution leaving the needle tip rather than relying on diffusion through the polymer mesh. Various degrees of fiber morphology retention have been reported in the literature using vapor crosslinking, likely due to the fact that it is difficult to control the amount and homogeneity of crosslinking. These variables are influenced by crosslinker transport, which is dependent on the mesh thickness. Diffusivity through the mesh is also decreased as the permeant interacts with functional groups on the polymer (crosslinks)[38] and as the crosslink density increases throughout the crosslinking process.[39] *In situ* crosslinking provides a more effective crosslinking strategy due to homogenous mixing at the needle tip prior to jet formation and fiber drawing.

Tensile Testing

The tensile mechanical properties of *in situ* crosslinked meshes were tested in an environmental testing chamber that maintained the temperature at 37 °C and humidity at 100% throughout testing to limit drying of the specimen during testing. The mechanical properties of 1X, 5X, and 10X crosslinked gelatin are summarized in **Figure 3** and **Table 2**. As the crosslinker ratio increases, the initial modulus and tensile strength increased, whereas the ultimate elongation decreased. These results are typical effects of increasing crosslining density in polymeric materials.[40, 41] A greater effect of crosslinker ratio was observed for 1X to 5X, compared with 5X to 10X. This result suggests that the amount of available crosslinking sites is reduced, which limits the effect of increasing crosslinker. Although the tensile properties of dry traditional glutaraldehyde crosslinked meshes reported in the literature are significantly higher than those reported here, it is important to note that the values reported in **Figure 4** are from hydrated specimens that more closely mimic the end use.[42]

***In vitro* Degradation**

Enzymatic degradation of the gelatin fibers was performed using a collagenase solution. Collagenase is known to cleave peptide bonds within the structure of gelatin.[43] As expected, an increase in crosslinker ratio, and therefore crosslinking density, resulted in reduced degradation rates, **Figure 4**. Full dissolution of the uncrosslinked gelatin was observed within 12 hours of

immersion within the collagenase solution. Gelatin 1X meshes experienced a loss of mechanical integrity at 4 days and underwent complete dissolution by 10 days. Gelatin 5X meshes and 10X meshes lost mechanical integrity by 16 and 22 days with full dissolution by 24 and 35 days, respectively. Although the effect of increasing crosslinker ratio from 5X to 10X on tensile properties was modest , the increase in degradation period between these two samples suggests that the observed increase in crosslink density (61% vs 91%) was able to modulate degradation. There was also an evident biphasic degradation of both the 5X and 10X meshes. This was attributed to dissolution of small diameter fibers first, followed by degradation of the larger diameter fiber population.[44] Finally, these results indicate improved crosslinking over the UV *in situ* crosslinking system reported by Lin et al., where 22% mass loss was observed after soaking in water for 24 hours.[37] The results of the *in vitro* degradation study demonstrate that crosslinking in the liquid phase of gelatin electrospinning results in a controlled degree of crosslinking, allowing for tunable degradation rates. SEM images of meshes at various points of the degradation study have been displayed in **Figure 5.** As these meshes were enzymatically degraded, it can be inferred that the structural stability would be maintained for prolonged periods in cell culture media that does not contain active enzymes. This is further confirmed by comparing Figure 5 to Figure 2, where improved fiber retention is exhibited after immersion in water at 37 °C for 1 week.

Cell Viability and Adhesion

Collagen-derived products such as gelatin are inherently bioactive with well characterized interactions with cells. Cell density and representative fluorescent images are displayed in **Figure 6**. Density on 1X *in situ* crosslinked meshes exhibited no significant difference to glutaraldehyde crosslinked meshes after 1 week of culture, with adhesion of 129 ± 20 and 118 ± 8 cells/mm^2, respectively *(p = 0.59)*. There was a statistically significant increase in cell density on the 5X *in situ* crosslinked meshes from 24 hours to 1 week *(p = 0.01)* Additionally, there was a statistically significant increase in cell density on the 5X *in situ* crosslinked meshes over traditional glutaraldehyde crosslinked meshes after 1 week of culture *(p < 0.01)*. In contrast, the gluteraldehyde-crosslinked displayed a significant decrease in cell density after 1 week *(p = 0.01)*. The 5X mesh results indicate that at this crosslinking density, the gelatin fibers retained sufficient bioactivity to support cellular adhesion and proliferation. It was hypothesized that the decreased cell adhesion to the 1X meshes was a result of the lower crosslinking density. Decreased crosslinking can result in increased swelling and a corollary reduction in modulus (supported by **Figure 3**). It is well established in literature that a decreased modulus reduces cell adhesion, however, it is important to note that the cells that do adhere are viable.[45]

Figure 7 displays the viability of hMSCs cultured on electrospun meshes over 24 hours and 1 week. Cells were viable on the 1X and 5X *in situ* crosslinked meshes, as well as the glutaraldehyde crosslinked mesh, over the course of the study. In contrast, the 10X mesh displayed reduced cell viability at both 24 hours and 1 week. An indirect viability study of the 10X meshes displayed no statistical difference as compared to TCPS viability. This suggests that the low cell viability was not due to residual HDI or other extractables. It was hypothesized that the reduced viability and cellular adhesion was due to reduced access of cellular integrins to RGD residues in the gelatin matrix.[8, 27, 37] Cell adhesion to collagen occurs through integrins $\alpha_1\beta1$, $\alpha2\beta1$, and, less prominently, through $\alpha_5\beta_1$ and $\alpha_V\beta_3$.[46, 47] Upon denaturation to form gelatin, the triple helical structure of collagen is lost with a corollary loss of integrin $\alpha_1\beta_1$ and $\alpha_2\beta_1$ affinity.[48, 49] The denaturation process also exposes previously hidden RGD sites within the resultant gelatin.[46] Therefore, it is commonly accepted that cell adhesion to gelatin is strongly dependent on these RGD residues and binding of the $\alpha_5\beta_1$ and $\alpha_V\beta_3$ integrins.[8,46, 48, 49] It is unlikely that the HDI crosslinking directly deactivates the RGD sequence directly due to the relatively slow reaction kinetics of HDI with arginine or aspartic acid as compared to lysine residues or water. However, we hypothesize that the high level of crosslinking in the 10X meshes reduced integrin-based interactions with RGD domains due to steric hindrance or limited accessibility.[8, 27, 37] Grover et al. also reported a decrease in cell adhesion on EDC-NHS crosslinked gelatin films (82% crosslinked), which is similar to the 10X composition presented here (91% crosslinked).[48] The high adhesion on 5X meshes (57% crosslinked) indicates that there may be an optimal threshold at which fiber morphology is retained and cellular interactions are enhanced.

Conclusions

This work describes a method for *in situ* crosslinking of gelatin to produce electrospun fibers with improved fiber morphology retention in water and tunable degradation rates. Given that fiber morphology plays a pivotal role in regulating cell behavior and mechanical properties, the improved retention in aqueous solutions indicate that *in situ* crosslinking provides a platform to fabricate effective tissue engineering scaffolds. *In situ* crosslinking enables a more effective crosslinking strategy than traditional vapor crosslinking due to homogenous mixing at the needle tip prior to jet formation and fiber drawing, allowing for a highly controlled system. Relationships between crosslinker ratio and degree of crosslinking, tensile mechanical properties, and rate of degradation were identified. As crosslinker ratio was increased, both degree of crosslinking and fiber retention increased in a controlled manner. The initial modulus and tensile strength also increased as the crosslinker ratio increased. Additionally, the capacity of gelatin mesh degradation to be tuned over a wide range was demonstrated. The versatility of this methodology allows for broad implementation with a variety of natural polymers (elastin, fibrinogen) with the requirement for implementation being the presence of primary amines. Further modulation of properties can be achieved by selecting diisocyanate crosslinkers with degradable sites, fluorophores, or pendant conjugation moieties (e.g. thiols). Selection of solvent can also influence crosslink length and helice formation with corrolary effects on scaffold mechanical

properties. Overall, *in situ* crosslinking of natural polymers during electrospinning provides a one-step fabrication method to achieve improved scaffolds for tissue engineering applications.

Acknowledgements

This work was supported by the Texas A&M University Diversity Fellowship and the National Science Foundation Graduate Research Fellowship Program under Grant No. 1252521. Any opinions, findings, and conclusions or recommendations expressed in this material are those of the author(s) and do not necessarily reflect the views of the National Science Foundation.

References

1. Q. P. Pham, U. Sharma and A. G. Mikos, *Tissue Engineering*, 2006, **12**, 1197-1211.
2. S. Ramakrishna, K. Fujihara, W. Teo, T. Lim and Z. Ma, *An introduction to electrospinning and nanofibers*, World Scientific Publishing Co. Pte. Ltd., Singapore, 2005.
3. J. Doshi and D. H. Reneker, *J Electrost*, 1995, **35**, 151-160.
4. K. Lee, H. Kim, Y. Ryu, K. Kim and S. Choi, *J Polym Sci, Part B Polym. Phys*, 2003, **41**, 1256-1262.
5. E. P. S. Tan, S. Y. Ng and C. T. Lim, *Biomaterials*, 2005, **26**, 1453-1456.
6. S.-C. Wong, A. Baji and S. Leng, *Polymer*, 2008, **49**, 4713-4722.
7. T. Stylianopoulos, C. Bashur, A. Goldstein, S. A. Guelcher and V. Barocas, *J Mech Behav Biomed Mater*, 2008, **1**, 326-335.
8. S.-C. Wu, W.-H. Chang, G.-C. Dong, K.-Y. Chen, Y.-S. Chen and C.-H. Yao, *Journal of Bioactive and Compatible Polymers*, 2011, **26**, 565-577.
9. V. Guarino, M. Alvarez-Perez, V. Cirillo and L. Ambrosio, *Journal of Bioactive and Compatible Polymers*, 2011, **26**, 144-160.
10. A. Farina, M. H. Fievet, F. Plassart, M. C. Menet and A. Thuillier, *Journal of Hospital Infection*, 1999, **43**, 293-297.
11. M. J. A. van Luyn, P. B. van Wachem, L. Olde Damink, P. J. Dijkstra, J. Feijen and P. Nieuwenhuis, *Journal of Biomedical Materials Research*, 1992, **26**, 1091-1110.
12. L. L. H. Huang-Lee, D. T. Cheung and M. E. Nimni, *Journal of Biomedical Materials Research*, 1990, **24**, 1185-1201.
13. D. M. Simmons and J. N. Kearney, *Biotechnology and Applied Biochemistry*, 1993, **17**, 23-29.
14. A. Jayakrishnan and S. R. Jameela, *Biomaterials*, 1996, **17**, 471-484.
15. C. E. Schmidt and J. M. Baier, *Biomaterials*, 2000, **21**, 2215-2231.
16. M. Skotak, S. Noriega, G. Larsen and A. Subramanian, *Journal of Biomedical Materials Research Part A*, 2010, **95A**, 828-836.
17. C. Barnes, C. Pemble, D. Brand, D. Simpson and G. Bowlin, *Tissue Engineering*, 2007, **13**, 1593-1605.
18. L. Buttafoco, N. Kolkman, P. Engbers-Buijtenhuijs, A. Poot, P. Dijkstra, I. Vermes and J. Feijen, *Biomaterials*, 2006, **27**, 724-734.
19. S. Panzavolta, M. Gioffrè, M. L. Focarete, C. Gualandi, L. Foroni and A. Bigi, *Acta Biomaterialia*, 2011, **7**, 1702-1709.
20. M. S. Kim, I. Jun, Y. M. Shin, W. Jang, S. I. Kim and H. Shin, *Macromolecular Bioscience*, 2010, **10**, 91-100.
21. K. Sisson, C. Zhang, M. Farach-Carson, D. Chase and J. Rabolt, *Biomacromolecules*, 2009, **10**, 1675-1680.
22. Y. Su and X. Mo, *Journal of Controlled Release*, 2011, **152, Supplement 1**, e230-e232.
23. S. Zhang, Y. Huang, X. Yang, F. Mei, Q. Ma, G. Chen, S. Ryu and X. Deng, *Journal of Biomedical Materials Research Part A*, 2009, **90A**, 671-679.
24. S. Y. Chew, R. Mi, A. Hoke and K. W. Leong, *Biomaterials*, 2008, **29**, 653-661.
25. C. H. Lee, H. J. Shin, I. H. Cho, Y.-M. Kang, I. A. Kim, K.-D. Park and J.-W. Shin, *Biomaterials*, 2005, **26**, 1261-1270.
26. A. S. Badami, M. R. Kreke, M. S. Thompson, J. S. Riffle and A. S. Goldstein, *Biomaterials*, 2006, **27**, 596-606.
27. C. A. Bashur, L. A. Dahlgren and A. S. Goldstein, *Biomaterials*, 2006, **27**, 5681-5688.
28. G. T. Christopherson, H. Song and H.-Q. Mao, *Biomaterials*, 2009, **30**, 556-564.
29. V. K. Sarin, S. B. H. Kent, J. P. Tam and R. B. Merrifield, *Analytical Biochemistry*, 1981, **117**, 147-157.
30. J. Ratanavaraporn, R. Rangkupan, H. Jeeratawatchai, S. Kanokpanont and S. Damrongsakkul, *International Journal of Biological Macromolecules*, 2010, **47**, 431-438.
31. C.-H. Huang, C.-Y. Chi, Y.-S. Chen, K.-Y. Chen, P.-L. Chen and C.-H. Yao, *Materials Science and Engineering: C*, 2012, **32**, 2476-2483.
32. W.-H. Chang, Y. Chang, P.-H. Lai and H.-W. Sung, *Journal of Biomaterials Science, Polymer Edition*, 2003, **14**, 481-495.
33. G. Tronci, A. T. Neffe, B. F. Pierce and A. Lendlein, *Journal of Materials Chemistry*, 2010, **20**, 8875-8884.
34. L. Meng, O. Arnoult, M. Smith and G. E. Wnek, *Journal of Materials Chemistry*, 2012, **22**, 19412-19417.
35. C. Tang, C. D. Saquing, J. R. Harding and S. A. Khan, *Macromolecules*, 2010, **43**, 630-637.
36. P. Gupta, S. R. Trenor, T. E. Long and G. L. Wilkes, *Macromolecules*, 2004, **37**, 9211-9218.
37. W.-H. Lin and W.-B. Tsai, *Biofabrication*, 2013, **5**, 035008.
38. S. C. George and S. Thomas, *Progress in Polymer Science*, 2001, **26**, 985-1017.
39. C. T. Reinhart and N. A. Peppas, *Journal of Membrane Science*, 1984, **18**, 227-239.
40. B. Ding, H. Y. Kim, S. C. Lee, C. L. Shao, D. R. Lee, S. J. Park, G. B. Kwag and K. J. Choi, *Journal of Polymer Science Part B: Polymer Physics*, 2002, **40**, 1261-1268.
41. S. S. Choi, J. P. Hong, Y. S. Seo, S. M. Chung and C. Nah, *Journal of Applied Polymer Science*, 2006, **101**, 2333-2337.
42. Y. Zhang, J. Venugopal, Z.-M. Huang, C. Lim and S. Ramakrishna, *Polymer*, 2006, **47**, 2911-2917.
43. Y. S. Choi, S. R. Hong, Y. M. Lee, K. W. Song, M. H. Park and Y. S. Nam, *Journal of Biomedical Materials Research*, 1999, **48**, 631-639.
44. W. Cui, X. Li, X. Zhu, G. Yu, S. Zhou and J. Weng, *Biomacromolecules*, 2006, **7**, 1623-1629.
45. T. Yeung, P. C. Georges, L. A. Flanagan, B. Marg, M. Ortiz, M. Funaki, N. Zahir, W. Ming, V. Weaver and P. A. Janmey, *Cell motility and the cytoskeleton*, 2005, **60**, 24-34.

46. G. E. Davis, *Biochemical and biophysical research communications*, 1992, **182**, 1025-1031.
47. M. Barczyk, S. Carracedo and D. Gullberg, *Cell Tissue Res*, 2010, **339**, 269-280.
48. C. N. Grover, J. H. Gwynne, N. Pugh, S. Hamaia, R. W. Farndale, S. M. Best and R. E. Cameron, *Acta Biomaterialia*, 2012, **8**, 3080-3090.
49. D. S. Tuckwell, S. Ayad, M. E. Grant, M. Takigawa and M. J. Humphries, *Journal of cell science*, 1994, **107**, 993-1005.

Figures

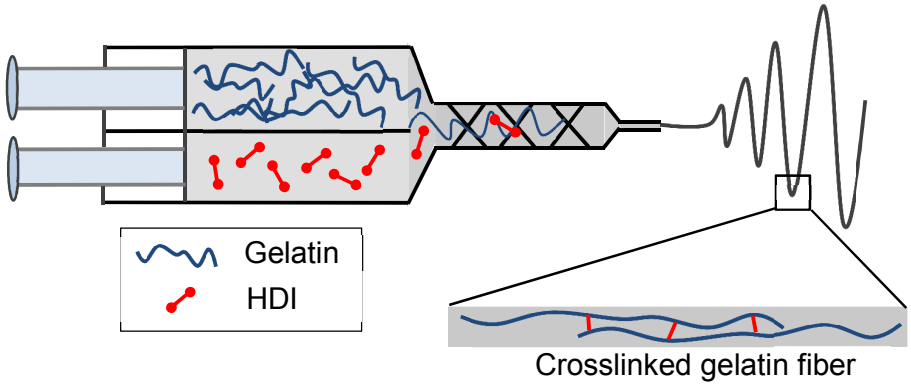

Figure 1: Schematic of double-barrel syringe setup for *in situ* crosslinking of gelatin during electrospinning.

Table 1: Degree of crosslinking of traditional glutaraldehyde crosslinked meshes and of *in situ* crosslinked gelatin with different crosslinker ratios (1X, 5X or 10X isocyanate to amine) and resulting percent increase in fiber diameter after a 1 week incubation in water.

Mesh	Degree of Crosslinking (%)	Increase in Fiber Diameter (%)
1X	$32 \pm 6^{+,\times}$	$170 \pm 13^{a,b}$
5X	$61 \pm 7^{+,*}$	9 ± 5^{a}
10X	$91 \pm 1^{\times,*}$	10 ± 4^{b}
Glutaraldehyde	57 ± 1	24 ± 9^{c}
5X	61 ± 7	9 ± 5^{c}

$^{+,\times,*,a,b,c,}$ indicate statistically significant differences between respective samples $p<0.05$

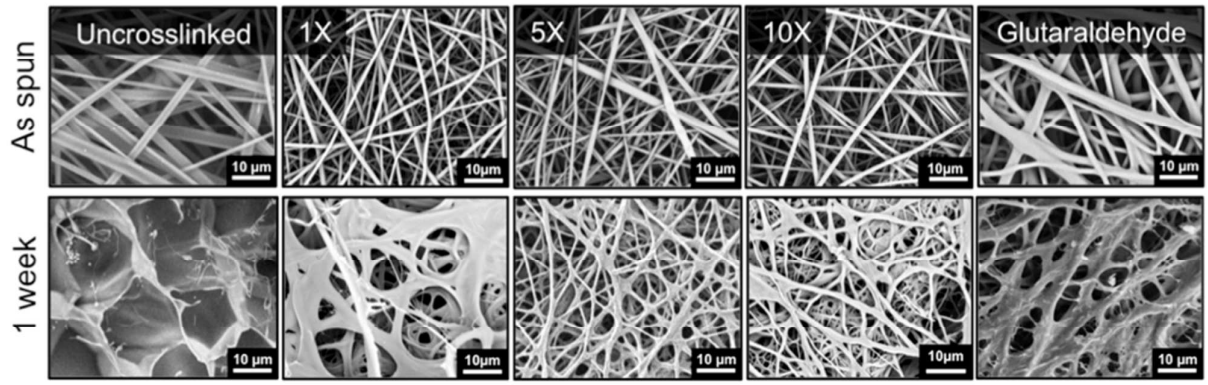

Figure 2: Scanning electron micrographs of *in situ* crosslinked gelatin with different crosslinker ratios (1X, 5X or 10X isocyanate to amine) compared to uncrosslinked and glutaraldehyde vapor crosslinked meshes, as-spun and after a 1 week incubation in water.

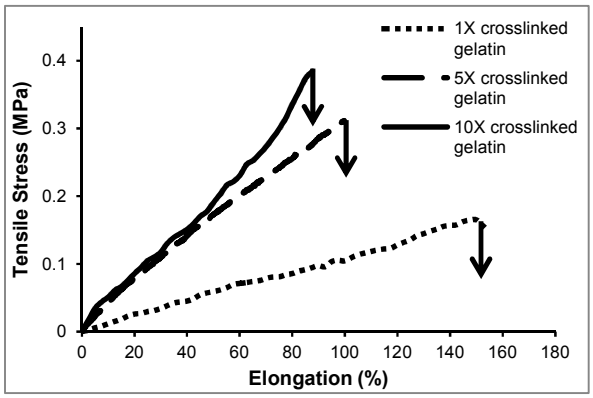

Crosslinker Ratio	2% Secant Modulus (MPa)	Ultimate Tensile Strength (MPa)	Elongation (%)
1X	0.4 ± 0.2	0.2 ± 0.1	150 ± 10
5X	0.7 ± 0.3	0.3 ± 0.1	100 ± 30
10X	0.8 ± 0.3	0.5 ± 0.2	90 ± 40

Figure 3/Table 1: Tensile properties of *in situ* crosslinked gelatin with 1X, 5X, or 10X crosslinker ratio (isocyanate to amine).

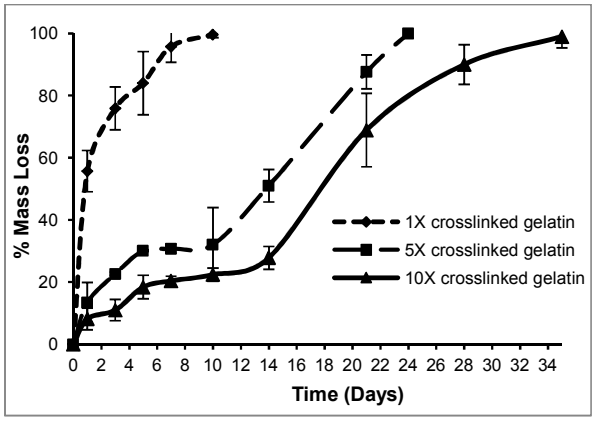

Figure 4: *In vitro* degradation of *in situ* crosslinked gelatin with 1X, 5X, or 10X crosslinker ratio (isocyanate to amine) in collagenase solution (0.02 units collagenase/mL).

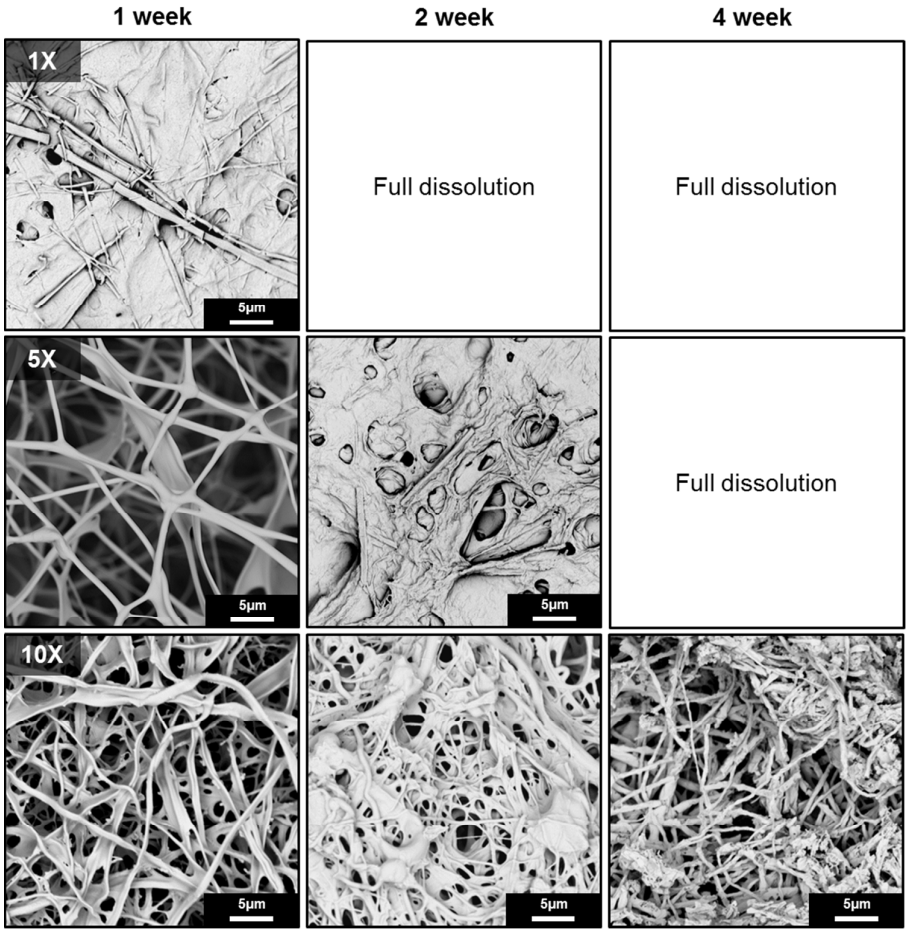

Figure 5: Scanning electron micrographs of *in situ* crosslinked gelatin with different crosslinker ratios (1X, 5X or 10X isocyanate to amine) after 1, 2 and 4 weeks incubation in collagenase solution at 37°C.

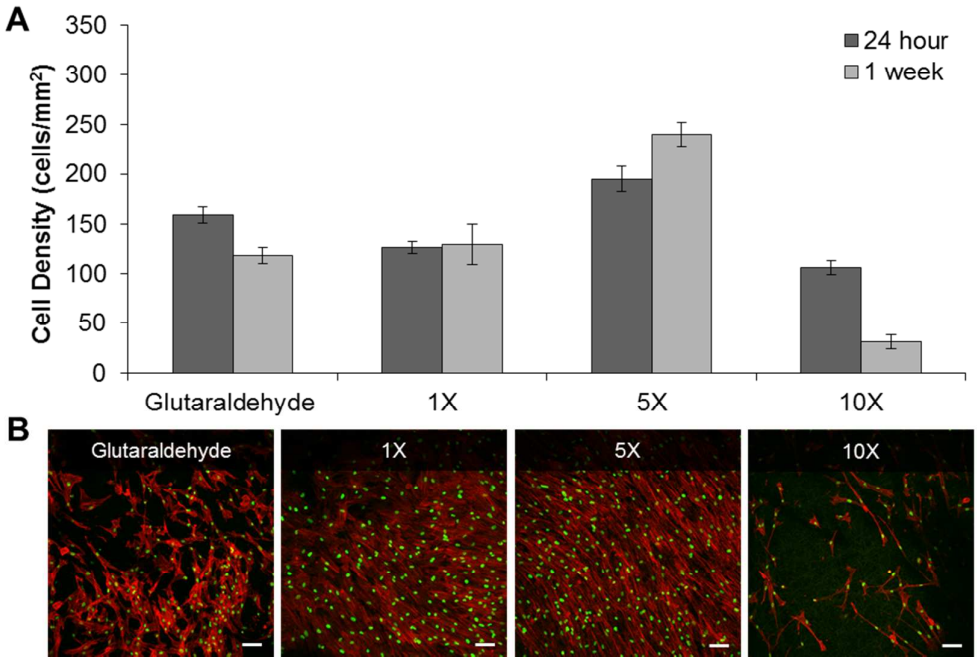

Figure 6: A) Adhesion of hMSCs to glutaraldehyde crosslinked gelatin and *in situ* crosslinked gelatin (1X, 5X. 10X) meshes. B) Representative fluorescent images of hMSCs cultured on glutaraldehyde crosslinked gelatin and *in situ* crosslinked gelatin (1X, 5X, 10X) after 1 week of culture. Scale bar = 100 µm

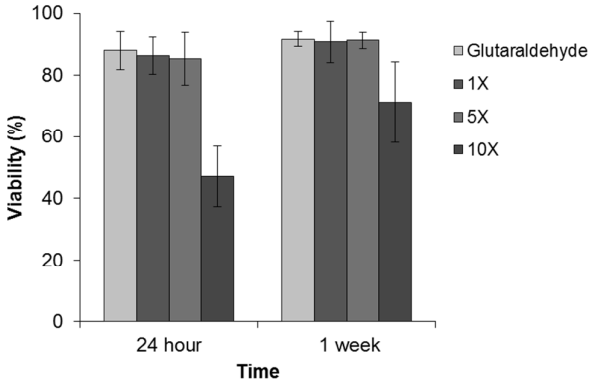

Figure 7: Viability of hMSCs on glutaraldehyde crosslinked gelatin and *in situ* crosslinked gelatin (1X, 5X, 10X) meshes.

Table of Contents Entry

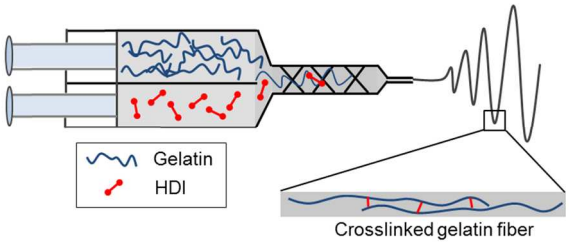

In situ crosslinking provides a method to crosslink gelatin during electrospinning enabling tunable degradation rates and displaying improved fiber morphology retention after implantation.